Blue-green emission of Pr^{3+} ions in $LiNbO_3$

2000 J. Phys.: Condens. Matter 12 709

(http://iopscience.iop.org/0953-8984/12/5/317)

J. Phys.: Condens. Matter **12** (2000) 709–718. Printed in the UK PII: S0953-8984(00)04497-0

Blue–green emission of Pr^{3+} ions in $LiNbO_3$

R Piramidowicz†, I Pracka‡, W Wolinski† and M Malinowski†§

† Institute of Microelectronics and Optoelectronics, ul. Koszykowa 75, 00-662 Warsaw, Poland
‡ Institute of Electronic Materials Technology, ul. Wólczynska 133, 01-919 Warsaw, Poland

E-mail: m.malinowski@imio.pw.edu.pl

Received 24 May 1999, in final form 19 October 1999

Abstract. The emission properties of the $^3P_0$ state of praseodymium ions in lithium niobate crystal have been studied. Blue–green emission at 510 nm corresponding to the $^3P_0 \rightarrow {}^3H_4$ transition in Pr^{3+}:$LiNbO_3$ crystals was generated after direct and up-conversion excitation with orange and infrared radiation around 920 nm. The up-conversion mechanisms were shown to be energy transfer and excited state absorption for orange and infrared excitation, respectively. The processes responsible for non-radiative relaxation of the $^3P_0$ state were also determined.

1. Introduction

Multifunction, compact, solid state lasers are designed to play an important role in the telecommunication, data storage and display technologies of the future. Recently, much attention has been focused on rare-earth (RE) doped lithium niobate ($LiNbO_3$) crystals as a laser material. Its excellent electro-optic, acousto-optic and nonlinear properties offer possibilities of developing commercial integrated laser devices and Q-switched, mode-locked, directly modulated and self-frequency doubling $LiNbO_3$ lasers have already been reported [1, 2]. Also the technology of RE doped $LiNbO_3$ planar waveguides offers a number of features that are not available in bulk devices, such as the preparation of grating structures for distributed feedback (DFB) (or distributed Bragg reflector (DBR)) resonators or quasi-phase matching [3]. Diode pumped channel waveguide lasers have been realized in Nd^{3+} [4] and Yb^{3+} [5] doped $LiNbO_3$. More recently, non-volatile holographic image recording in praseodymium-doped lithium niobate has also been demonstrated [6].

Thus, there has recently been a rapid growth of interest in studying the optical and spectroscopic properties of rare-earth ions in $LiNbO_3$; and Nd^{3+} [7], Pr^{3+}[8], Dy^{3+} [9, 10], Ho^{3+} [11], Er^{3+} [12] and Tm^{3+} [13, 14] doped $LiNbO_3$ crystals have been characterized. Trivalent praseodymium (Pr^{3+}) is an interesting activator, since its energy levels offer a variety of emission transitions extending from near ultraviolet (UV) to infrared (IR). Low-temperature absorption and emission spectra of the Pr^{3+} ion in $LiNbO_3$ were investigated in [8, 15] and most of the Stark energy levels of $LiNbO_3$:Pr^{3+} were determined in [16], however, the luminescence properties of this material are still not fully described. It was shown that in $LiNbO_3Pr^{3+}$, differently from other oxide materials, the main channel of radiative de-excitation is through the $^1D_2$ state and that luminescence from the $^3P_0$ state is very weak and its decay is very fast.

§ Corresponding author: Institute of Microelectronics and Optoelectronics PW, ul. Koszykowa 75, 00-662 Warsaw, Poland.

0953-8984/00/050709+10$30.00

There also exist significant differences between the optical properties of Pr^{3+} in $LiNbO_3$ and $LiTaO_3$ which have very similar crystal and electronic structure [17, 18].

These reported results stimulated our further spectroscopic investigation of Pr^{3+} in $LiNbO_3$ for the purpose of establishing the properties that are important for the $^3P_0$ emission in the blue–green region.

One of the methods for increasing the optical pump efficiency of Pr^{3+} doped laser materials is the sensitization with trivalent ytterbium ions (Yb^{3+}) [19]. The Yb^{3+} ions exhibit a strong and broad absorption band centred at about 960 nm and can be easily pumped with IR laser diodes. Recently, this configuration has been used for single diode up-conversion pumping of the Yb^{3+} sensitized Pr^{3+} ZBLAN glass fibre laser [20, 21], but $Yb^{3+} \rightarrow Pr^{3+}$ energy up-conversion in $LiNbO_3$ has never been, to our knowledge, studied.

We present a series of new measurements of the $^3P_0$ luminescence in Pr^{3+} and $Pr^{3+} + Yb^{3+}$ activated $LiNbO_3$ under various excitation conditions, including direct one photon (OP), up-conversion and two wavelength pumping.

2. Experimental methods

The $LiNbO_3$:Pr^{3+} crystals were obtained by the Czochralski method at the ITME Laboratory in Warsaw. $LiNbO_3$ samples with concentrations of 0.1, 0.5 and 1% of Pr^{3+} ions and doubly doped $LiNbO_3$:0.1%Pr^{3+} + 0.8%Yb^{3+} and $LiNbO_3$:0.5%Pr^{3+} + 0.8%Yb^{3+} samples were grown from a congruent melt (Li/Nb = 0.94) parallel to the $\langle c \rangle$ direction. For optical measurements the samples were cut out perpendicularly to the optical c-axis and were double side optically polished. Absorption spectra at temperatures of 10 and 300 K were measured with a Bruker IFS 113V FT-IR spectrometer. Fluorescence and excitation spectra were obtained using a tunable visible laser operating with Coumarine 480 and Rhodamine 640 dyes, pumped by the second and third harmonics of a Continuum Surelite Nd:YAG. For pulsed excitation in the IR region the output wavelength of a tunable laser operating with DCM dye, pumped by a frequency doubled Continuum Surelite Nd:YAG laser, was 4155 cm^{-1} downshifted by stimulated Raman scattering (SRS) in a gaseous H_2 cell. Continuous wave (CW) excitation in the blue region was achieved by a ILA-120 3 W argon ion laser. The spectra were recorded using a GDM-1000 monochromator with dispersion of 11 cm^{-1} mm^{-1} and detected by a RCA C 31034-02 cooled AsGa photomultiplier. Data acquisition was obtained using a SR 400 photon counting system controlled with a PC computer. Fluorescence lifetime measurements were made using a SR 430 multichannel analyser. Sample cooling was provided by a closed circuit He optical cryostat allowing a temperature variation between 10 and 300 K.

3. Results

3.1. Analysis of optical spectra

It was observed, see figure 1, that under blue OP excitation at 476 nm the luminescence of the $LiNbO_3$:Pr^{3+} was mostly from the $^1D_2$ level. Even at low temperatures the short wavelength emission at about 510 nm, which corresponds to the $^3P_0 \rightarrow {}^3H_4$ transition, is very weak. From the absorption spectra measured at 10 K, when only the ground state is populated, and from the low-temperature emission spectra, the positions of Stark energy levels were assigned and are presented in table 1. It should be noted that even at 10 K the optical transitions of Pr^{3+} ions in $LiNbO_3$ are, as proved by site selective spectroscopy [15], inhomogeneously broadened. Thus, some of the individual Stark components are not well resolved and the energy levels

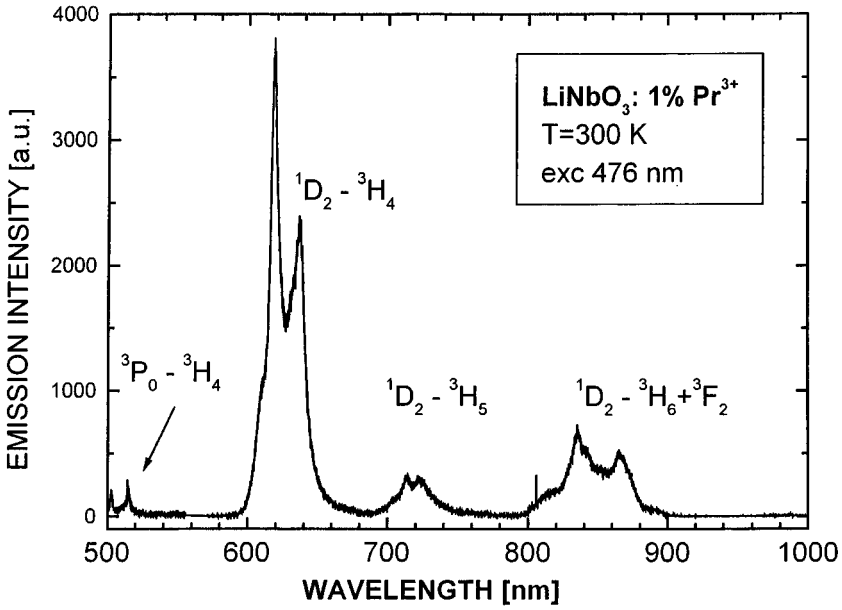

Figure 1. The emission spectrum of $LiNbO_3$:Pr^{3+} crystal obtained at 300 K after 476 nm CW excitation.

Table 1. Energy levels of Pr^{3+} in $LiNbO_3$ measured at 10 K.

$[S'L'J']$	E (cm^{-1})
$^3P_2$	21 607, 21 676, 21 760
$^1I_6$	
$^3P_1$	20 546, 20 574, 20 685[a]
^3P	19 880
$^1D_2$	16 190, 16 274, 16 586
$^1G_4$	9430, 9563, 9689, 9815, 9835, 10 074, 10 098[a]
$^3F_4$	6826, 6862, 6884, 6925, 6967
$^3F_3$	6316, 6362, 6398, 6469, 6499
$^3F_2$	5012, 5030, 5086, 5115
$^3H_6$	4141, 4230, 4344, 4370, 4560[a], 4690[a], 4768
$^3H_5$	2153, 2210, 2241, 2354, 2515, 2579
$^3H_4$	0, 35, 93, 147, 385, 495[a]

[a] Denotes less accurate results.

reported here are good within about 10 cm^{-1}. This could also explain, in some degree, large differences between the energy level positions presented in table 1 and reported in [16]. The results on the energies of Stark levels of Pr^{3+} in $LiNbO_3$ listed in table 1 shows that the $^3P_0$ level is considerably lower in energy than in other crystals, to our knowledge lithium niobate is the only matrix where the $^3P_0$ energy is less than 20 000 cm^{-1}. The position of the $^1I_6$ levels is not easy to determine using low-temperature absorption data because $^3H_4 \rightarrow {}^1I_6$ transitions are spin forbidden and weak relative to the close lying, strong, spin allowed $^3H_4 \rightarrow {}^3P_J$ lines. The weak absorption band near 475 nm is probably due to $^1I_6$ levels, although strong inhomogeneous broadening and vibronic transitions to ^3P_J make precise assignment difficult. Calculated $^1I_6$ levels position has been reported in [16].

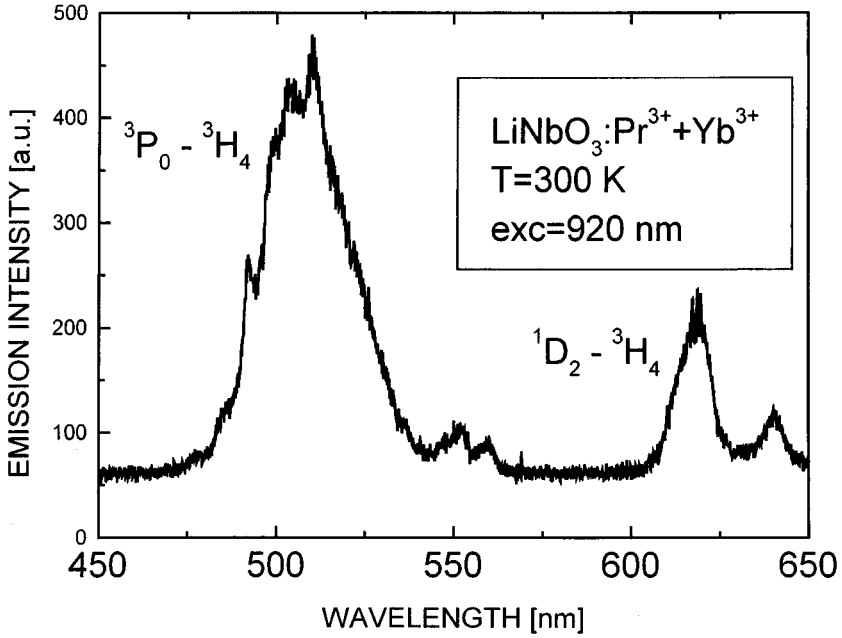

Figure 2. Up-conversion excited, blue–green and red fluorescence spectrum of $LiNbO_3:Pr^{3+}+Yb^{3+}$ crystal after IR (920 nm) pumping at 300 K.

When studying praseodymium fluorescence in $LiNbO_3$ it is interesting to note that, different visible emission spectra were obtained depending on the excitation scheme. In single Pr^{3+}-doped $LiNbO_3$ at 10 K, a weak emission from the $^3P_0$ state was observed, similar to the case after OP excitation, under pulsed laser pumping around 16 190 cm^{-1} which is the energy of the lowest $^1D_2$ level. In the same sample relatively strong emission from the $^3P_0$ manifold was observed between 10 and 300 K for excitation wavelength in the 880–950 nm band. The excitation spectrum of this anti-Stokes fluorescence has its maximum around 900 nm and is presented in the lower part of figure 3. A square intensity dependence of the up-converted $^3P_0$ emission on IR pumping power was determined.

In the next step, we studied the possibility of sensitization of the $^3P_0Pr^{3+}$ luminescence by codoping the crystals using Yb^{3+} ions and pumping them with the IR radiation. It was observed that $LiNbO_3:Pr^{3+}$ + Yb^{3+} emits much more efficiently in the green than singly doped crystals under the studied excitation conditions. In figure 2 the up-conversion excited at 300 K blue–green fluorescence spectrum corresponding to the $^3P_0 \rightarrow {}^3H_4$ transition is presented and in figure 3 IR excitation spectrum of this emission is shown.

3.2. Fluorescence dynamics

Figure 4 shows the low-temperature fluorescence decay profiles of the $^3P_0$ manifold in the investigated samples.

Decay curves of the $^3P_0$ fluorescence of praseodymium in $LiNbO_3$ after OP excitation were found to be non-exponential, see figure 4(a), (b) and (e). The non-exponential features were more obvious in the 1% sample. The long time part of the decays measured at 10 K in the

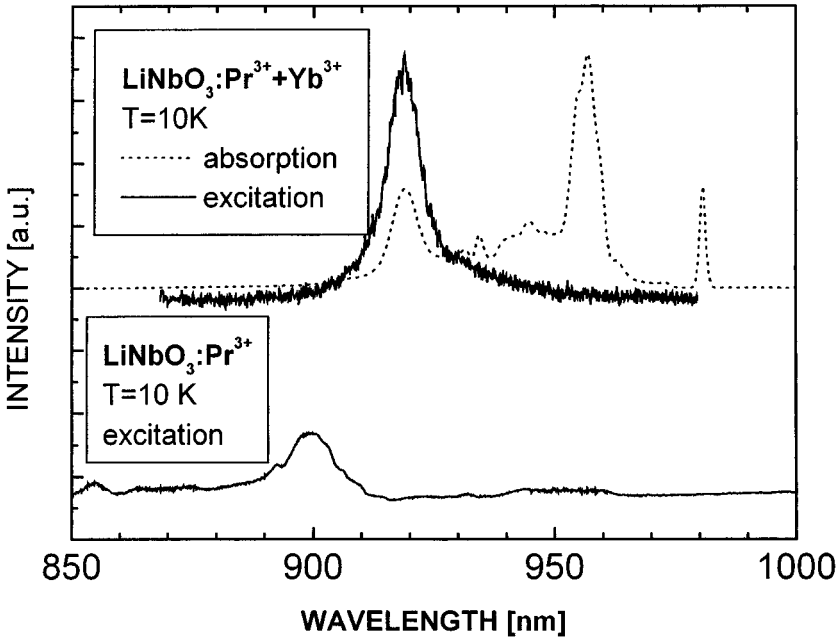

Figure 3. Excitation spectrum of the $^3P_0$ blue–green emission and absorption spectrum of the $LiNbO_3:Pr^{3+} + Yb^{3+}$ and an excitation spectrum of the $^3P_0$ emission in singly activated $LiNbO_3$:1% Pr^{3+} sample measured at 10 K.

0.1% and 1% Pr^{3+} sample indicate lifetimes of 0.52 and 0.19 μs, respectively. Decay of the directly OP pumped $^3P_0$ fluorescence in $LiNbO_3$:0.1%Pr^{3+} + 0.8%Yb^{3+} was non-exponential with a long time constant of 0.12 μs. Following excitation of the $^3P_0$ level rise times of 0.5 μs and 0.2 μs were observed in the decay profile of the $^1D_2$ emission in the 0.1% and 1% Pr^{3+}-doped sample, respectively and were attributed to the non-radiative decay from the $^3P_0$ level to the $^1D_2$ level.

The temporal evolution of the anti-Stokes emission resulting from the excitation of the $^1D_2$ manifold was studied in $LiNbO_3$:1%Pr^{3+}. The transient decay curves demonstrated a short rise-time component characteristic of energy-transfer up-conversion (ETU) followed by decay having a time constant of about 0.25 μs, see figure 4(d). We observed that the intensity of the up-converted emission varies quadratically with the orange pump energy. The blue–green emission transient of $LiNbO_3$:1%Pr^{3+} obtained by IR pumping has a quite different behaviour, the decay has no observable rise-time and is similar to that after OP direct excitation, see figure 4(c). As in the case of orange excitation, intensity of the $^3P_0$ emission had a quadratic dependence on the IR pump intensity.

Finally, the effect of IR laser density on the fluorescence decay in 1% Pr^{3+} doped $LiNbO_3$ was examined. The increase of the $^3P_0$ decay time at high IR excitation density was observed. The roughly determined lifetime increased from about 0.2 μs measured under 1 J cm^{-2} laser excitation to about 2.5 μs for the 15 J cm^{-2} laser excitation density.

The $^2F_{5/2}$ decay curves of the Yb^{3+} ions in the investigated samples are presented in figure 5. It can be seen that the decay of ytterbium, see figure 5(c), is nearly exponential with a long time constant of 1.07 ms. With the presence of Pr^{3+} ions in the crystal the initial part of the decays became non-exponential, see figure 5(a).

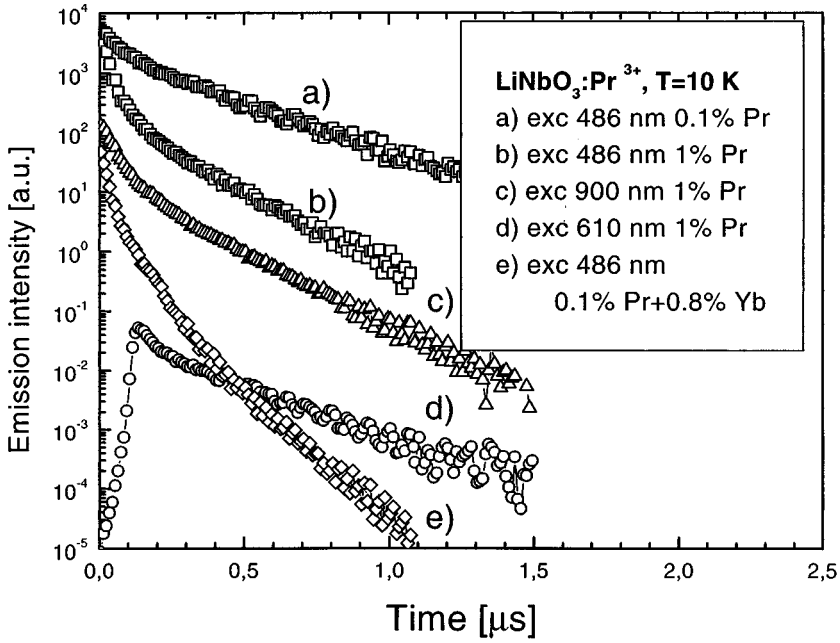

Figure 4. Low-temperature fluorescence decay curves for the $^3P_0$ excited state of Pr^{3+} in: (a) $LiNbO_3$:0.1% Pr^{3+} after 486 nm excitation; (b) $LiNbO_3$:1% Pr^{3+} after 486 nm excitation; (c) $LiNbO_3$:1% Pr^{3+} after 900 nm excitation; (d) $LiNbO_3$:1% Pr^{3+} after 610 nm excitation; (e) $LiNbO_3$:0.1% Pr^{3+} + 0.8%Yb^{3+} after 486 nm excitation.

4. Discussion

The weakness of emission from the $^3P_0$ level in $LiNbO_3$:Pr^{3+} is surprising, since the energy gap to the underlying $^1D_2$ level is about 3300 cm^{-1} which corresponds to the multiphonon decay probability W_{nr} of about 5×10^3 s^{-1} [12]. Thus, the measured fluorescence lifetime of 0.52 μs should not differ significantly from the calculated radiative lifetime. Neither non-radiative relaxation via intersystem crossing, observed in Pr^{3+} doped Y_2O_3 [22] and (La, Pr)Ti_2O_7 [23] could be active in $LiNbO_3$, as praseodymium 4f5d levels are lying at about 35 000 cm^{-1}, that is well above ^3P_J levels.

The observed non-exponential decay of the $^3P_0$ state is an indication that efficient energy transfer is taking place even in low the concentration 0.1% Pr^{3+} sample. The cross relaxation mechanisms that are likely to occur in the $LiNbO_3$:Pr^{3+} system were analysed with the aid of the determined positions of the energy levels. One of the possible resonant processes, due to the relatively low-lying $^3P_0$ state, of these types is denoted as $^3P_0 \rightarrow {}^1G_4 = {}^3H_4 \rightarrow {}^1G_4$.

The next step in our investigation was to determine the strength and character of this donor–acceptor interaction in $LiNbO_3$:Pr^{3+}. Assuming that the donor–donor transfer is negligible at low temperatures the time dependence of the $^3P_0$ emission could be described by the Inokuti–Hirayama [24] equation of the form

$$\ln I/I_0 + t/\tau_0 = \frac{4\pi n_A R_{01}^3}{3}(X_{01}t)^{3/s}\Gamma(1 - 3/s) \tag{1}$$

where τ_0 is the lifetime of the $^3P_0$ state at low concentration, n_A is the number of acceptors per unit volume, and R_{01} and X_{01} are the nearest-neighbour separation and donor–acceptor interaction rate, respectively, s identifies the nature of the interaction and Γ is the gamma

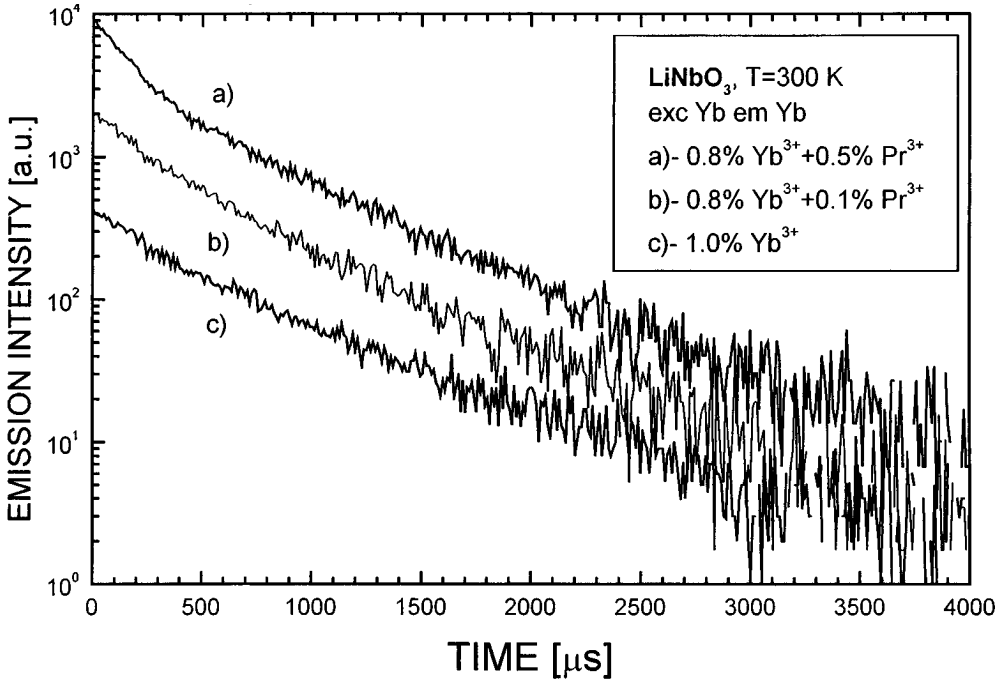

Figure 5. Yb^{3+} emission decays at 1.06 μm in: (a) $LiNbO_3$:0.5%Pr^{3+} + 0.8%Yb^{3+}; (b) $LiNbO_3$:0.1%Pr^{3+}+0.8%Yb^{3+}; and (c) $LiNbO_3$:1%Yb^{3+} crystals measured at room temperature after pulsed excitation of Yb^{3+} ions at 920 nm.

function. From figure 6 it can be seen that for the appropriate choice of s a plot of $\ln I/I_0 + t/\tau_0$ against $t^{3/s}$ gives a straight line. In the case of $LiNbO_3$:Pr^{3+} the plot can be best fitted for $s = 6$ indicating the dipole–dipole nature of the interaction. The best fit is obtained with using a radiative lifetime value of 4.2 μs. This is much longer than the lifetime of 0.52 μs measured for low concentrated $LiNbO_3$:0.1%Pr^{3+} confirming the predominantly non-radiative character of this metastable state. The presented analysis yields the nearest-neighbour donor–acceptor transfer rate X_{01} to be 0.16×10^6 s^{-1}, which is about two orders of magnitude higher than the cross relaxation rate of 1.0×10^3 s^{-1} for Pr^{3+} ions in 0.1%Pr^{3+}:YAG at 12 K [25].

The radiative lifetime calculated here for $^3P_0$ is in a good agreement with the value of $\tau_0 = 4$ μs deduced from the quantum efficiency of this state which was experimentally determined in [8] to be 0.13. It is also interesting to note that the radiative lifetime of the praseodymium $^3P_0$ level in $LiTaO_3$, calculated theoretically using Judd–Ofelt [26, 27] theory, was 4.5 μs [17].

Thus, it could be believed that, due to the specific energy level positions of Pr^{3+} ions in $LiNbO_3$, very efficient cross-relaxation quenching of the emission via the $^1G_4$ state takes place in this material. In order to qualitatively confirm this mechanism the blue–green fluorescence decays were recorded after pulsed two colour laser pumping simultaneously in the $^1G_4$ and $^3P_0$ manifolds. With the 20 μJ at 462 nm and 180 μJ at 900 nm excitation the $^3P_0$ decay was nearly exponential with a time constant of about 3 μs which is much longer than the lifetime of 0.52 μs measured after one colour direct excitation in the low concentration sample. This could be interpreted in terms of reduction of the $^3H_4$ ground state population and build up of the $^1G_4$ state population with growing IR pumping. In the 0.1% sample the absorption

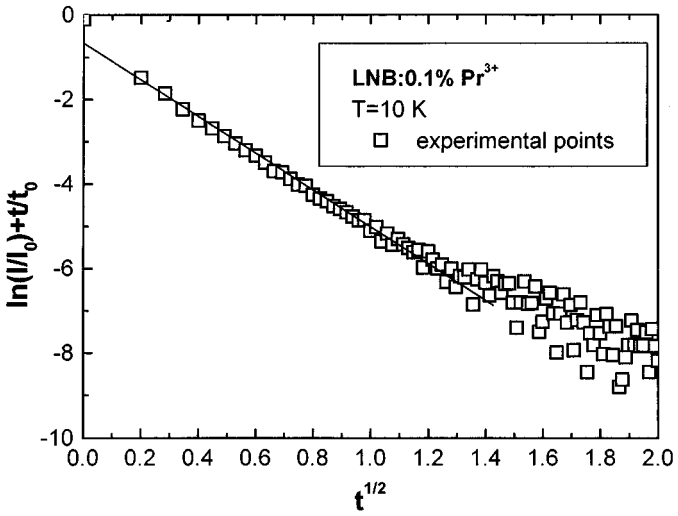

Figure 6. Plot of $\ln(I/I_0) + t/\tau_0$ against $t^{1/2}$ for 0.1% Pr^{3+} doped $LiNbO_3$ at 10 K. The straight line approximation indicates a cross-relaxation rate $X_{01} = 0.16 \times 10^6\ s^{-1}$ for ions in the $^3P_0$ state.

coefficient of the $^1G_4$ state at 10 K is 0.008 cm^{-1} and with the IR laser excitation energies of the order of 180 μJ focused to the spot of 10^{-5} cm^2 the $^1G_4$ densities are about 10^{20} cm^{-3} corresponding to about 10% excitation. This results in the saturation and lower efficiency of the $^3P_0 \rightarrow {}^1G_4 = {}^3H_4 \rightarrow {}^1G_4$ cross relaxation pathway.

The quadratic dependence of the $^3P_0$ blue up-converted emission on the orange and IR pump intensity indicates, in both cases, a two-photon excitation process.

The blue–green $^3P_0$ emission after orange pumping could be related to the following energy transfer up-conversion mechanism; $^1D_2 \rightarrow {}^1G_4 = {}^1D_2 \rightarrow {}^3P_2$ where the excess energy of 522 cm^{-1} is released.

After IR pumping in the singly activated Pr^{3+}:$LiNbO_3$ system, as in YLF, YAG, and GGG crystals [28, 29], the up-conversion process was two step absorption; the first step was identified to be a non-resonant $^3H_4 \rightarrow {}^1G_4$ transition and the second step—ESA from the lower Stark level of the $^1G_4$ state to $^1I_6$ and ^3P_J levels of Pr^{3+}. 900 nm excitation of the $^3P_0$ emission corresponds to transitions between lower levels of $^1G_4$ and $^3P_1$ levels, see table 1. Weaker lines in the 850–880 nm band could be transitions to $^1I_6$. In the Yb^{3+} sensitized $LiNbO_3$:Pr^{3+} sample, the IR pumped blue fluorescence is much more intense, and from the identical shape of the excitation spectra of the Pr^{3+} emission and Yb^{3+} $^2F_{5/2}$ absorption presented in figure 3 results that the first step is essentially GSA $^2F_{7/2} \rightarrow {}^2F_{5/2}$ transition followed by energy transfer to populate the $^1G_4$ manifold of Pr^{3+}. The second step is ESA from the $^1G_4$ levels to the $^3P_J + {}^1I_6$ levels. This explains the absence, in the up-conversion excitation spectrum, see figure 3, of transitions having energies lower than this corresponding to the 920 nm line as they will terminate below the $^3P_0$ level. The 920 nm ESA transition itself suggests the non-resonant character of this absorption step, probably to the phonon band of the $^3H_4 \rightarrow {}^3P_0$ transition or existence, at about 20 300 cm^{-1}, of not detected $^1I_6$ levels between $^3P_0$ and $^3P_1$ states. Figure 7 shows a relevant part of the Pr^{3+} and Yb^{3+} energy level diagrams and the proposed two-ion excitation scheme. Three ion processes like stepwise energy transfer and cooperative excitation are less probable and could be ruled out by the quadratic intensity dependence of the up-converted fluorescence. From the energy level scheme of $LiNbO_3$ we found that GSA of

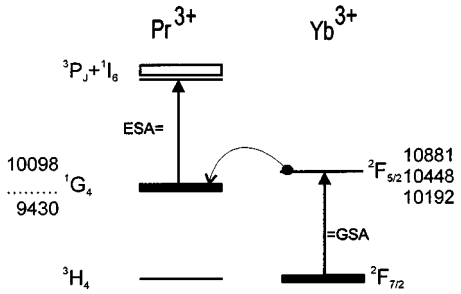

Figure 7. Diagram of the energy levels for Pr^{3+} and Yb^{3+} ions in $LiNbO_3$ crystal and up-conversion excitation mechanism.

Pr^{3+} and Yb^{3+} ions does not overlap in the IR region, the strong $^2F_{7/2} \rightarrow {}^2F_{5/2}$ absorption band of Yb^{3+} is located at a slightly shorter wavelength allowing phonon assisted, about 100 cm^{-1} mismatch, energy transfer from Yb^{3+} to Pr^{3+} to occur. This mechanism also explains the high efficiency of up-conversion at room temperature in the Yb^{3+} activated YAG:Pr^{3+}. The efficiency of back-transfer from Pr^{3+} to Yb^{3+} is reflected by additional reduction of the ^3P fluorescence lifetime in the presence of Yb^{3+} ions, see figure 4(e). From the energy level scheme presented in figure 7 the most probable mechanism is a resonant cross relaxation between an excited Pr^{3+} ion and Yb^{3+} in the ground state; $^3P_0(Pr^{3+}) + {}^2F_{7/2}(Yb^{3+}) \rightarrow {}^1G_4(Pr^{3+}) + {}^2F_{5/2}(Yb^{3+})$. This process also participates in the creation of the $^1G_4$ state population.

After excitation of the $^3P_0$ level the $^1D_2$ level is populated only by non-radiative decay which is confirmed by the observed, concentration dependent rise-time in the $^1D_2$ fluorescence decay wave form. Thus, the differences in the shape and relative intensity of the $^1D_2$ and $^3P_0$ emissions observed under direct, see figure 1, and up-conversion pumping, see figure 2 could be discussed in terms of the excitation of Pr^{3+} ions in non-equivalent crystal field sites, characterized by different degrees of coupling to the lattice and resulting in different non-radiative decay rates.

As in all the above discussed processes, of cross relaxation and up-conversion excitation of the $^3P_0$ fluorescence, the $^1G_4$ manifold is involved as an intermediate state and the population of blue–green emitting ions is indirectly controlled by ions in the $^1G_4$ state. This is also confirmed by the observed effect of IR laser density on $^3P_0$ fluorescence decay.

5. Conclusions

We have investigated the processes responsible for the excitation and relaxation of the $^3P_0$ level of praseodymium in $LiNbO_3$ crystals. It has been shown that extremely efficient quenching of the $^3P_0$ emission takes place in the investigated system after one photon excitation. It was also observed that $^3P_0$ emission is relatively much stronger after IR up-conversion excitation. It is concluded that this unusual optical behaviour of Pr^{3+} ions in $LiNbO_3$ is related to the very low position of the $^3P_0$ level which allows for nearly resonant cross relaxation via $^1G_4$ levels but also allows for quasi-resonant ESA from the $^1G_4$ to take place.

References

[1] Johnson L F and Ballman A A 1969 *J. Appl. Phys.* **40** 297
[2] Becker P, Brinkmann R, Dinand M, Sohler W and Suche H 1992 *Appl. Phys. Lett.* **61** 1257
[3] Sochtig J, Groß R, Baumann I, Sohler W, Schutz H and Widmer R 1995 *Electron. Lett.* **31** 551

[4] Plissi M V and Wilson M G F 1994 *IEE Proc. Optoelectron.* **141** 195
[5] Jones J K, De Sandro J P, Hempstead M, Sheppard D P, Large A C, Tropper A C and Wilknson J S 1994 *Proc. School of Physics 'Rare Earth Doped Optical Waveguides' (Les Houches, 13–26 June 1994)*
[6] Bai Y S, Neurgaonkar R R and Kachru R 1997 *Optics Lett.* **22** 334
[7] Loro H, Voda M, Jaque F, Munoz-Santiuste J E and Garcia-Sole J 1995 *J. Appl. Phys.* **77** 5929
[8] Lorenzo A, Bausa L E and Garcia Sole J 1995 *Phys. Rev.* B **51** 16 643
[9] Lorenzo A, Camarillo E, Murrieta H S, Alvarez E, Caldino V G, Hernandez A, Voda M, Jaque F and Garcia Sole J 1996 *Opt. Mater.* **5** 251
[10] Malinowski M, Myziak P, Piramidowicz R, Pracka I, Lukasiewicz T, Surma B, Kaczmarek S, Kopczynski K and Mierczyk Z 1996 *Acta Phys. Pol.* **90** 181
[11] Lorenzo A, Bausa L E, Sanz J A and Garcia Sole J 1996 *J. Phys.: Condens. Matter* **8** 5781
[12] Amin J, Dussardier B, Schweizer T and Hempstead M 1996 *J. Lumin.* **69** 17
[13] Nunez L and Cusso F 1993 *J. Phys.: Condens. Matter* **5** 5301
[14] Łuczyński Z, Łukasiewicz T, Pracka I, Surma B and Malinowski M 1995 *J. Appl. Spectrosc.* **62** 66
[15] Lorenzo A, Jaffrezic H, Roux B, Boulon G, Bausa L E and Garcia Sole J 1995 *Phys. Rev.* B **52** 6278
[16] Munoz-Santiuste J E, Lorenzo A, Bausa L E and Garcia Sole J 1998 *J. Phys.: Condens. Matter* **10** 7653
[17] Solkólska I, Ryba-Romanowski W, Golab S, Lukasiewicz T and Swirkowicz M 1997 *J. Phys.: Condens. Matter* **9** 5217
[18] Ryba-Romanowski W, Sokólska I and Golab S 1997 *Appl. Phys. Lett.* **70** 686
[19] Johnson L F and Guggenheim H 1971 *Appl. Phys. Lett.* **19** 44
[20] Baney D M, Yang L, Ratcliff J and Kok Wai Chang 1995 *Electron. Lett.* **31** 1842
[21] Ping Xie and Gosnell T R 1995 *Letters* **20** 1014
[22] Guyot Y, Moncorge R, Merkle L D, Pinto A, McIntosh B and Verdun H 1996 *Opt. Mater.* **5** 127
[23] Diallo P T, Boutinaud P, Mahiou R and Cousseins J C 1998 *J. Alloys Compounds* **275–277** 307
[24] Inokuti M and Hirayama F 1965 *J. Chem. Phys.* **43** 1978
[25] Xingkun Wu, Dennis W M and Yen W M 1994 *Phys. Rev.* B **50** 6589
[26] Judd B R 1962 *Phys. Rev.* **127** 750
[27] Ofelt G S 1962 *J. Chem. Phys.* **37** 511
[28] Malinowski M, Joubert M F and Jacquier B 1994 *Phys. Rev.* B **50** 12 367
[29] Malinowski M, Piramidowicz R, Sarnecki J and Woliński W 1999 *J. Phys.: Condens. Matter* **10** 1909